

A Compact, Lightweight, Fast-Response Preferential Oxidation Reactor for PEM Automotive Fuel Cell Applications.

Castaldi*, Marco J., Boorse, R. Samuel, Roychoudhury, Subir, Menacherry#, Paul V., and Pfefferle, William C.

Precision Combustion, Inc., 410 Sackett Point Road, North Haven, CT 06473

1. ABSTRACT

Proton exchange membrane fuel cells (PEMFC) are well suited for automotive applications due to their high power density and relatively low operating temperature. The hydrogen required can either be supplied directly or be generated on-board the vehicle by reforming hydrocarbon or alcohol fuels. Practical considerations favor the latter allowing the utilization of current fuel production and distribution networks. One of the problems associated with onboard generation of hydrogen is the co-production of carbon monoxide (CO). Current PEMFC's are extremely sensitive to the presence of (CO) and require its removal to less than 10 ppm in the reformat stream entering the fuel cell. Towards this goal, a highly active and selective catalytic reactor based on an atypical catalyst substrate design has been developed for the Preferential or Selective Oxidation of CO (PROX or SOX). PROX reactor design and performance data, produced with a variety of catalyst and washcoat formulations and reactor operating parameters, are reported. The Microlith[®] substrate reactor may be pictured as a series of catalytically coated screens each with ultra-short channel lengths, high cell density and low thermal mass, resulting in extremely high heat and mass transfer rates. This allows the reactor to operate with space velocities as high as 440,000 hr⁻¹. The observed result is a very compact reactor with rapid transient response, improved selectivity, and lower required loadings of precious metal catalysts. A full-scale prototype reformer demonstrated power densities greater than 30 kW/liter of catalyst volume, which is consistent with sub-scale experiments performed.

*To whom correspondence should be addressed. Email: mcastaldi@precision-combustion.com

2. INTRODUCTION

Proton exchange membrane fuel cells (PEMFC), being developed for eventual replacement of IC engines, operate at relatively low temperatures, usually below 100 °C. The hydrogen fuel required can either be supplied directly or be generated on-board the vehicle by reforming of hydrocarbon fuels like methanol, natural gas and gasoline. At the low operating temperatures the Pt anodes are highly sensitive to trace amounts of carbon monoxide (CO) in the hydrogen feed. Preferential oxidation (PROX) of CO is a simple and cost effective technique for removing trace CO contaminants. Small size, weight and cost as well as fast transient response and startup of the on-board fuel processing system, including the PROX reactor, are key to the successful integration of this technology for automotive applications. This requires significant advances over current technology and represents unique and difficult development challenges. Improvements in substrate performance, reactor design and catalysts are needed to meet the projected requirements – such as those for the Partnership for Next Generation vehicles (PNGV). The remaining discussion will focus on the development of a non-equilibrium, high space velocity reactor capable of meeting or exceeding the PNGV targets for fuel cell vehicle application.

3. BACKGROUND

In order to achieve the sub-10 ppm CO levels needed for PEM fuel cell application, CO conversions of 90% or more are needed in the PROX unit. Representative values of shifted reformat were taken from The Fuel Cell Handbook 5th edition with O₂ addition to produce an O₂/CO ratio of 1.2. Equilibrium calculations and CO conversions done for a range of inlet temperatures for the shifted reformat show that thermodynamics do not favor 100% selectivity of O₂ to convert CO and reverse water gas shift reactions need to be avoided. Even at temperatures of 25°C, the calculations show that all the O₂ is converted with most reacting with H₂ to form water. From that temperature forward, the reverse water-gas shift reaction occurs, which works against the reactor designer trying to produce a CO free effluent. Figure 1 shows how quickly the CO conversion drops with rising temperature. At 75°C CO conversion is 90%, whereas at 125°C conversion is 75% and 175°C conversion drops to 35%. In fact CO production, due to the reverse water gas shift reaction, begins to occur by 210°C. However the levels of H₂, CO₂ and H₂O are only slightly affected by the temperature rise. For example, at 75°C H₂ concentration is 52.2% and at 175°C the H₂ level is relatively unchanged at 51.9%. This indicates that low operating temperatures are desirable to keep CO conversion high to produce a CO free effluent. Yet, high temperatures are preferred for higher CO oxidation reaction rates, thus allowing reactors to be reasonably small in size. The equilibrium values for this reaction have been determined to help define the operating window for allowable CO removal. One way to achieve high CO conversions at temperatures near 200°C, where the kinetics of the CO oxidation reaction are sufficiently fast, is to operate a reactor at non-equilibrium conditions. One possible scheme for this type of operation is the use the Microlith reactor described above, which is a short contact time (microsecond scale) reactor similar to others[1].

While short contact time reactors allow effective operation away from the equilibrium constraints, appropriate choice of catalysts is important to facilitate the desired reaction. In addition, considerations for reactor design will focus on a variety of other parameters, such as space velocity, pressure drop and staging. The most probable reactions that can occur within the reactor for this type of composition are:



The catalyst formulation chosen will have to be selective toward CO oxidation (reaction 1) over methane and water production reactions (reactions 3 and 4), as well as be active at low temperatures where the reverse rate of reaction 2 is slow. The formulation will also need to be highly active for reaction 1, thus allowing the use of near stoichiometric amounts of O₂. Stoichiometric amounts of O₂ are desirable to keep the selectivity toward CO conversion high. Any O₂ remaining after conversion of CO will react with H₂, thus decreasing the effectiveness of the reactor.

A. Substrates

Current PROX reactors use pellet or monolith-based [2] substrates. However, these substrates have both low mass transport and heat transport properties especially when operating under mass transfer

limited conditions. Also, they have a high thermal mass, which results in greater time constants for temperature equilibration. Substrates with high transport properties have been explored at Argonne National Laboratories but the impact on pressure drop for these substrates is not available.

B. PROX Catalysts

In general, different precious metal catalysts have been found to be highly selective for the PROX reaction. Different workers have reported the use of supported Ru, Rh [3], Pt [4,5] and Au [6] for this reaction. A general understanding of these systems is that at temperatures before the onset of the CO lightoff the surface is covered with adsorbed CO. As the temperature is increased the fraction of the surface covered with CO decreases, and this opens up sites for oxygen adsorption and subsequent reaction. Above a certain temperature the fraction of CO occupying the surface decreases even further and hydrogen chemisorbs and reacts on the surface in competition with CO, reducing the selectivity towards CO oxidation. Therefore, a common feature of all these systems is that there exists a window of operation in temperature between the lightoff curves for CO and H₂, the object being to operate at a catalyst temperature sufficient for high activity of CO oxidation (for reduced size of catalytic reactor), but below that for significant consumption of the hydrogen. This is illustrated schematically in Figure 2. The inlet temperature to the PROX reactor should ideally be less than or equal to the Low Temperature Water Gas Shift Reactor exit temperature generally found just upstream of the PROX reactor. This would allow easy transition, without heat exchangers or control schemes, into the PROX reactor.

The CO oxidation activity on these catalysts has also been reported to be enhanced by moisture in some cases, and surface formate species have been postulated as reaction intermediates in this reaction [7]. Also depicted in Figure 1 are the CO and H₂ lightoff curves, which are shifted both in absolute temperature and relative to each other for different catalyst formulations depending on the relative adsorption energies on the different catalyst surfaces. This results in different temperature windows and optimum catalyst temperatures, which need to be identified for different catalyst formulations. Selective oxidation of CO in hydrogen over different catalysts has been extensively examined. CuO-CeO₂ mixed oxide catalysts have been studied by Avgouropoulos, et al [8] and Gasteiger, et al have explored bimetallic PtSn catalysts [9]. Gold supported on manganese oxides, prepared via use of an organo gold complex in the liquid phase, albeit with stability concerns of Au/MnOx in H₂ has been reviewed by Tanaka, et al [6]. Watanabe et al have studied Mordenite-supported noble metal catalysts [10] with Watanabe et al also having examined Pt/ γ -Al₂O₃ and Au/ α -Fe₂O₃ [11]. Oh and Sinkevitch have reported Ruthenium/alumina and rhodium/alumina for high CO conversion below 100°C [3]. Platinum supported on zeolite and mordenite for selectivity approaching 100% at high H₂ concentrations has been observed by Watanabe et al [12]. Catalyst surface coverage and reaction kinetics for the PROX reaction over Pt/ γ -Al₂O₃ and Au/ α -Fe₂O₃ has been described by Gasteiger et al [13].

While most of these formulations have been studied over beaded or monolithic catalysts, the current paper explores the use of some of the more promising formulations in reactors based on unique short contact time substrates. A brief review of the catalysts and reactor designs reported follows.

C. Reactor Design

Since the oxidation of CO and H₂ are highly exothermic ($\Delta H = -67$ kcal/mol and -58 kcal/mol, respectively), control of reactor temperature becomes a critical issue. A calculation of the adiabatic temperature rise for a typical reformat stream exiting a Low Temperature Shift reactor with 5000 ppm CO and with 2500 ppm added O₂ was ~ 45 °C (assuming 100% selectivity to CO oxidation). Therefore, depending on the operating window of the specific catalyst formulation, the catalyst temperature may have to be controlled prior to the onset of bulk mass transfer limited operation. This can be accomplished by varying the inlet temperature to the PROX reactor to account for the temperature rise along the length of the reactor and/or use of a staged reactor with inter-stage cooling. The Microlith catalyst substrate developed is especially suited in applications where control of reactor temperature is critical. As discussed in the next section, the combination of low thermal mass and extremely high convective transport rates of the Microlith metal monoliths provides the ability of maintaining a more uniform gas-catalyst temperature profile than with other catalyst substrates such as conventional monoliths or pellets. This enables the reactor to run closer to the gas phase temperature than conventional monolithic or pellet bed reactors before the onset of bulk mass transfer controlled reaction. There are many groups working on reactor design to develop a PROX reactor for PEM fuel cell use, including the major automotive manufacturers. For example General Motors has a patent application for a multi-stage, isothermal PROX reactor.

D. Microlith technology

In competition with those groups, a Microlith metal monolith technology, patented and trademarked Microlith[®], being developed by PCI [14], is a novel reactor engineering design consisting of a series of high cell density, short channel length, and low thermal mass metal monoliths. Conventional monolith substrates have long channel lengths relative to the channel diameters, and a boundary layer becomes fully developed within the first few channel diameters. The Microlith grids have very short channels, thereby avoiding substantial boundary layer buildup and resulting in significantly enhanced heat and mass transfer rates for improved catalyst-gas interaction. The results of a Computational Fluid Dynamics (CFD) analysis shown in Figure 3 illustrates the difference in boundary layer thickness between a conventional monolith and the Microlith metal monolith substrate. The effectiveness of this catalyst substrate has been demonstrated in automotive lightoff converter applications [15,16] The heat and mass transfer coefficients depend on the boundary layer thickness, which is a function of the length scale of the catalyst support. For a honeycomb monolith a fully developed boundary layer is present over a considerable length of the device. This limits the rate of mass transfer and thus limits conversion under mass transfer-limited conditions. Convective heat exchange with the gas phase also follows the same principles and the heat transfer coefficient is also strongly dependent on the boundary layer buildup. The Microlith technology avoids such boundary layer limitation by replacing the long channels of a conventional monolith with a series of short channel length substrates, each short enough to avoid substantial boundary layer build-up.

E. Effect of improved mass transport

Under bulk mass transfer-limited operation the rate of conversion is equal to the rate of diffusion to the surface of the catalyst. Mass transfer is a function of the geometric surface area (external surface of the catalyst) and the mass flux to the catalyst surface is given by the following expression:

$$-Q dC = k_c C dA \quad \dots\dots\dots (1)$$

where: Q is the volumetric flow rate,
 C is the concentration of the reacting species,
 k_c is the mass transfer coefficient, and
 A is the total geometric surface area (GSA).

From this it follows that the conversion, c , over a catalyst of area A is

$$c = 1 - \exp(-k_c A/Q) \quad \dots\dots\dots (2)$$

This expression only accounts for diffusion of a single species to the catalyst surface, which is a good assumption when conversion is limited by the diffusion of one reactant species to the surface of the catalyst. Since k_c and GSA for the Microlith are approximately higher by factors of 10 and 2 respectively over a typical monolith, the conversion (per unit surface area) over a Microlith substrate at a given flow rate is much higher. This equation shows the important role of mass transfer on reaction rate.

F. Comparative analysis of Microlith and monoliths due to support interactions

The preceding section compared the bulk mass transfer limited conversion on the Microlith substrate. The comparison is extended to washcoated substrates (i.e. high surface area supports) in the following analysis via the Thiele model, which is the ratio of the surface reaction rate under surface rate controlling conditions versus under diffusion rate controlling within porous solids. The effect of the mass transfer coefficient on observed reaction rates for the Microlith substrate is compared to a 400 cpsi (cells per square inch), 1 in. long conventional monolith substrate incorporating the same washcoat/catalyst formulation including the effect of diffusion in the porous catalyst supports.

Porous catalyst washcoats on the two substrates were modeled using the Thiele Model for intraparticle diffusion [17,18] and a bulk mass transfer rate based on the mass transfer coefficient, k_c , and a bulk gas phase concentration C of the reacting species. *Note:* This analysis considered a differential reactor, i.e., C was assumed constant over the length of the reactor. While the actual application will utilize an integral reactor, the results from the differential reactor are illustrative in that they show the effect of mass transfer coefficient on the observed reaction rate across a differential section of reactor. Since in many applications, the pressure drop across the catalytic reactor is an important consideration, this analysis compares reactors having approximately equal pressure drop. This results in a Microlith-based reactor, having less than 1/10th the volume of a 400cpsi, monolith based reactor.

From this analysis,

$$C_s = k_c * A * C / [(\Phi * D/L^2) + k_c * A] \quad \dots\dots\dots(1)$$

where C_s is the concentration of the reacting species i at the washcoat periphery, Φ is the Modified Thiele Modulus, L is a length parameter, in this case the washcoat thickness, D is the effective diffusivity of the gas molecules in the pores and A is the geometric surface area (GSA) per reactor.

Therefore, the observed rate of reaction (per reactor) is given by the following expression,

$$\text{rate} = k_c * A * C / [1 + k_c * A / (\Phi * D / L^2)] \quad \dots\dots\dots(2)$$

The parameters used to model the conventional monolith and Microlith substrate are shown in Table 1. The analysis has been done for an isothermal case, i.e., neglecting the effects of intra-particle heat transfer. Although intra-particle heat transfer will change the slope of the lightoff curves, it is believed that the results will be qualitatively very similar showing the delayed onset of mass transfer on the Microlith catalyst substrate compared to the conventional monolith substrate. This analysis shows that the enhanced transport properties of the Microlith catalyst substrate results in a delayed onset of mass transfer limited conversion. The magnitude of this is illustrated in the following example for the specific case of CO oxidation over a Pt/ γ -alumina catalyst. Reaction temperatures corresponding to the modified Thiele Moduli, Φ , were calculated. Activation energy values and pre-exponential factor were taken from Nibbelke et. al. [19]. The results are shown in Figure 4.

The differences between the Microlith catalyst substrate reactor and the conventional monolith reactor can be illustrated by considering the operation at a few conditions in Figure 4. (As mentioned above, the analysis considered two reactors of equal pressure drop, therefore the Microlith substrate reactor has about 1/9th the GSA and less than 1/10th the volume of the conventional monolith reactor).

At the temperature corresponding to points A1 and A2, the reaction is kinetically limited on both substrates. Therefore, the observed reaction rate on the monolith substrate is approximately 9 times greater on the conventional monolith than on the Microlith reactor (because the rate is proportional to the amount of catalyst present which was assumed proportional to the GSA).

At the temperature corresponding to points B1 and B2, the rate is still close to kinetically limited on the Microlith substrate (the broken line corresponds to kinetic operation), whereas it starts to get significantly pore diffusion limited on the conventional monolith reactor. The observed reaction rate on the Microlith substrate reactor is approximately 1/5th that for the conventional monolith reactor.

At the temperature corresponding to points C1 and C2, the reaction starts to become pore diffusion limited on the Microlith substrate, whereas it is almost bulk mass transfer limited on the conventional monolith reactor. The observed rate on the Microlith reactor is almost 1/2 that on the monolith reactor. *Note:* Since under these flow conditions the conversion across the Microlith substrate reactor is directly proportional to the number of elements, the same conversion as on the monolith reactor can be achieved in an Microlith reactor by doubling the number of elements. This would still result in a 5-fold size advantage with an accompanying increase in pressure drop.

At the temperature corresponding to points D1 and D2, the reaction is bulk mass transfer limited on both the substrates. The Microlith substrate reactor has roughly the same conversion as the conventional monolith reactor (from eqn. 2, conversion depends on the product of geometric surface area, A , and the mass transfer coefficient, k_c , which is slightly higher on the Microlith substrate reactor in this case). Therefore, equivalent conversion is achieved in an Microlith substrate reactor having less than 1/10th the volume of the conventional monolith reactor and equivalent pressure drop. *Note:* The leveling out in the reaction rates results because the analysis did not account for the dependence of D on temperature which results in a very gradual increase in mass transfer limited conversion with temperature.

The results show that mass transfer limited operation is shifted to higher temperatures on the Microlith substrate because of the enhanced mass transfer. The temperature difference between the Microlith substrate and the monolith for equivalent reaction rates was ~35 °C before the onset of significant mass transfer limitation (points A, B in Figure 4). Under bulk mass transfer limited conversion the Microlith reactor had approximately the same conversion as the 400 cpsi, 1" long monolith although it was less than 1/10th the size. Although these results were obtained for a particular catalyst washcoat, they will be qualitatively similar for other catalyst washcoat combinations. This analysis shows that the enhanced transport properties of the Microlith substrate results in onset of mass transfer limited conversion at a higher temperature compared to long channel monoliths, and higher conversion for equivalent pressure drop at a fraction of the volume under mass transfer limited operation.

G. Experimental Validation

This result was experimentally verified. Figure 5 shows the CO conversion and lightoff for a 0.1 in. deep Microlith reactor and a 1 in. deep, 400 cpsi monolith incorporating the same catalyst and washcoat formulations. This shows that the Microlith reactor has a higher lightoff temperature but equivalent

conversion as the monolith reactor, consistent with the Thiele analysis prediction. The Microlith catalyst substrate also shows slightly higher maximum CO selectivity consistent with better temperature control. The data therefore shows that the Microlith reactor can give equivalent performance with 1/10th the volume of a conventional monolith substrate, demonstrating the significant size reduction possible for the PROX component.

H. Substrate Coating

In an effort to make the reactor easy to manufacture and durable for automotive use the substrate material chosen is a high temperature metal alloy. This alloy needs to be capable of withstanding rapid thermal gradients and constant vibrations for extended periods of time, on the order of thousands of hours. In order to make use of the short contact time reactor concept as a catalytic support, the substrate needs to accept a coating layer onto which the catalytically active metal will be dispersed. This presents a challenge since the metal substrates and the catalyst supports, comprised of a porous ceramic layer, create a material mismatch. Additionally, most microlith designs rely on substrate configurations that have a very high radius of curvature of the substrate surface. Thus, in order to keep the catalyst on the surface, the support layer must adhere to a substrate that has a very different thermal expansion coefficient and has sharp edges and tight bends. In order for such a support coating to be successful, it must be both adherent and coherent while simultaneously having a relatively high surface area. Among the important considerations in achieving adhesion and cohesion are the thickness of the coating, the surface area of the starting powders, the powder to binder ratio, the specifics of the slurry formulation, drying and calcination times and temperatures. In general, because coating thickness is critical, coating techniques have been developed to yield as uniform a coating thickness as possible. This helps prevent areas of excessive thickness which can lead to spallation as well as increasing the uniformity of subsequent catalyst layers.

Once an adherent support layer has been established on the substrate, the catalyst is deposited. This is usually accomplished by impregnation of the support layer with a solution that contains precursors of the catalyst metal as metal salts. The amount of catalyst that is loaded on the support layer is a function of the volume of precursor solution that is absorbed into the porous layer and the precursor concentration in the solution. To control loading, two methods can be employed. One way, known as incipient wetness, is to completely wet support layer, filling all of its voids, until no more liquid can be held by the support layer. This method usually generates a coating with a constant catalyst to support loading ratio. The second approach is to deposit a known quantity of precursor per unit area even if the support coating is not become fully wet. This method usually generates a known catalyst loading to GSA ratio independent of support coating thickness.

From the standpoint of reactor design, in order to implement the short contact time substrate there is the need for expression of catalyst characteristics in terms that can be easily used by reactor designers. Especially important are terms, which allow comparison between different catalyst types and formulations. Towards this end, some definitions of catalyst loading that will be useful in our discussion of PROX reactors will be introduced in the following section.

Mesh area A_m is the macroscopic area of the mesh element that is used in a reactor. Thus, a mesh that is 10 inches by 10 inches has a mesh area of 100 in². Measurement of mesh area is simply by ruler.

Geometric surface area, GSA, is the surface area of the substrate metal usually expressed in square inches. The GSA of a particular substrate is highly dependent on the specifics of the mesh design and thus, GSA is usually calculated from design parameters such as wire diameter, and mesh weave density.

Specific surface area, SSA, refers to the physical surface area of the porous catalyst support material. Conventionally, SSA is expressed in units of in² per gram of support and can range widely from 5 to 500 depending on the specific materials used. SSA is usually obtained by a BET nitrogen physisorption measurement.

Catalyst Dispersion, D_c , is an expression of the percentage metal exposed to the reactants (both on the external surface and in the pores) and is usually considered equivalent to catalytically active metal. It is expressed as atoms (or grams) of exposed metal divided by atoms (or grams) of total metal loaded on the support. Dispersion is measured by chemisorption of a probe molecule onto catalytically active metal sites. For the purpose of describing the amount of catalyst that is contained in a reactor and how efficiently that catalyst is being used, we define a quantity called Active Site Index, ASI which is the catalyst metal loading per mesh area times the dispersion.

$$ASI = (L/A_m) * D_c$$

ASI, then, gives a measure of the catalytically active metal per mesh area and increases with greater dispersion and/or greater loading. ASI can then be used to give the reactor designer a comparison between different catalysts and between different reactor designs. For instance, by simply multiplying ASI by the total mesh area in the reactor we can get a measure of the total catalytically active metal in a particular reactor configuration and use that to differentiate between competing designs.

3. RESULTS AND DISCUSSION

As discussed above, the formulations with the highest intrinsic activity for the CO oxidation reaction are derived from the platinum group metals (PGM). To that extent, a number of formulations were examined for lightoff temperature for the reaction $\text{CO} + \frac{1}{2}\text{O}_2 = \text{CO}_2$ (1) (which is a measure of activity), selectivity toward CO conversion, and maximum CO conversion achievable.

The main objective was to develop a formulation that gave high conversion at low temperature and was active primarily for the CO oxidation reactions. The tests were done with O_2/CO ratio of 1:1 and a reactor space velocity of $440,000 \text{ hr}^{-1}$, which will allow small reactor design possible. A supported platinum catalyst formulation showed the highest CO conversion, at 47%, and selectivity, at 60%, albeit with a high lightoff temperature. A supported rhodium catalyst had the lowest lightoff temperature although the conversion and selectivity were both about 35%, which was significantly lower than the Pt formulation. The ruthenium catalyst had very low CO oxidation activity with significant methanation at the higher temperatures. Palladium had almost no oxidation activity until 250°C with minimal conversion thereafter. The Ru and Pd results are consistent with reported activity for preferential CO oxidation[20]. While other researchers have reported high activity at unusually low temperatures for gold-based catalysts, the Au/MnO/alumina formulation examined here did not show any appreciable performance, even at the higher temperatures. This could be due to the much higher space velocities examined here versus the studies at lower space velocities done by others which were in the range of 8000 to $20,000 \text{ hr}^{-1}$ [21,22,23] (space velocities in this paper are 20 times higher).

From the comparisons done under these conditions, the platinum catalyst was chosen as the formulation for the reactor optimization studies. This formulation allowed examination of a wide window of temperature operation with no observed methanation. A CO inhibition effect was observed at higher inlet concentrations of CO leading to a delayed lightoff but higher maximum conversions. One cause for the CO inhibition is likely the strong adsorption of CO on the Pt surfaces. Due to the high concentration of H_2 in the reactants, competing reactions ($\text{H}_2 + \frac{1}{2}\text{O}_2$) as well as H_2 adsorption on the surface occurs. One possible mechanism could be CO strongly adsorbs onto a Pt site, then H_2 reacts with the adsorbed CO to form H_2O , leaving behind carbon on the surface, which O_2 may then react with that carbon to re-form into adsorbed CO. Clearly, there is a competition between CO adsorption, H_2 reaction with adsorbed CO or O_2 or both and the ability for the O_2 to react with the carbon to form CO_2 and subsequently desorb to free the site for another reaction. Because of the CO inhibition effect, a set of inlet parameters must be optimized to give high conversions of CO with high selectivity, yet have a low lightoff temperature to avoid running into reverse water gas shift reaction limitations. Figure 6 shows a comparison between CO inlet concentrations and amount of O_2 available for reaction, defined as λ ; where $\lambda = 2 \cdot \text{O}_2/\text{CO}$. Higher λ indicates more O_2 and $\lambda > 1$ results in excess oxygen for the CO to CO_2 reaction, thus leaving O_2 remaining to react with H_2 once the CO has been exhausted.

Analysis of the data in Figure 6 indicates there is a CO inhibition effect on the platinum catalyst somewhere between the 500 and 1000 ppm CO inlet concentrations. A comparison between the 1000 ppmV CO inlet (■) and the 500 ppm CO inlet (○) for the same oxygen availability, $\lambda = 4$, shows a higher lightoff temperature for the higher CO concentration sample. While the lightoff temperatures are higher, the maximum achieved conversion and selectivity are higher for the 1000 ppm case. Further analysis shows that higher λ 's lead to more complete conversion but generally lower selectivity, as expected. Another observation is that higher λ 's are required with lower CO concentrations to achieve greater than 99% CO conversion. In the temperature range studied, it is evident that higher CO concentrations can unexpectedly affect the reactions. In Figure 6b, the 1000 ppm CO (■) sample has poor selectivity at low and high temperatures. At low temperatures, the CO oxidation reaction is probably inhibited, while at high temperatures the catalyst is less discriminating between reacting CO or H_2 . Also notice the rank order of selectivity versus λ for the two CO concentration levels. For the 1000 ppm concentration sample, selectivity gets better as λ is increased whereas the opposite is true at the 500 ppm level tests. These types of effects are important in reactor design with varying CO inlet concentrations and may lead to cross over

into an inhibition regime, where lightoff and selectivity are affected. Lastly, it is clear in Figures 6a and 6b that the temperature corresponding to maximum conversion does not correspond to maximum selectivity. The maximum selectivity occurs at lower temperatures, usually before the reactor is fully lit off. This would suggest the catalyst surface might be initially covered by one of the reactants (CO or O₂) at the low temperatures where it is easy for the other reactant to combine with the adsorbed species. As temperature is increased, reaction rates increase, allowing greater conversion, although with decreasing selectivity, indicating possible competition between the initial reactant (CO or O₂) on the surface and H₂. Obtaining and defining a wide operating window therefore presents a significant challenge.

In an effort to explore the operation window for the catalyst, additional comparisons between CO inlet concentration of 10,000 ppm (●) and 5000 ppm (○) were done to determine if much higher CO concentrations had the same effect as that at the lower levels. Figure 7 shows the CO conversion comparison for the 5000 and 10,000 ppm inlet concentrations versus temperature. Lightoff trends were similar to the low concentration studies, in that the 10,000 ppm sample had a more gradual, higher temperature lightoff as compared to the 5000 ppm sample. This suggests the inhibition mechanism is the same over large changes in CO inlet concentrations. Note that for the data reported in Figure 7, $\lambda = 2.0$, which is lower than in the low CO concentration study discussed above in Figure 6 and may be why maximum CO conversions were the same. An interesting observation is the ability to achieve approximately 85% conversion here with $\lambda = 2$ whereas at the lower CO concentrations, λ 's of 4 or higher were needed to achieve that amount of conversion. This suggests competition between CO and H₂ for O₂, and at the higher CO concentrations CO is more effective in competing for the available O₂ than at the lower CO concentrations.

The selectivity results, also shown in Figure 7, give an indication as to the type of mechanism dominating for the CO oxidation reaction. Notice the divergence between the selectivities at the low temperatures, before light off is complete. The high concentration, while has a lower conversion rate, has a much higher selectivity than the 5000 ppm sample. This clearly indicates the CO initially adsorbs onto the catalyst surface prior to reaction and the inhibition effect is due to this CO adsorption. Not until a temperature of near 250°C, when significant activity is taking place on the 10,000 ppm sample, do the selectivities approach each other. The 5000 ppm sample has a selectivity curve that indicates the amount of CO present at that concentration level is not enough to completely cover the catalyst sites, therefore there is probably a competition of reactions occurring from the beginning. Again the temperature of maximum conversion does not correspond to that of maximum selectivity.

To elucidate the mechanism for CO oxidation, an oxygen stoichiometry study was done for the Pt catalyst discussed above. The CO concentration was kept at 5000 ppm and the oxygen stoichiometry, λ , was varied from 1 to 3 and the PROX activity and selectivity in each case was investigated over a suitable range of temperature. The results are shown in Figure 8. As can be seen, with increasing λ the maximum selectivity decreases but the maximum CO conversion increases. The maximum CO conversion was seen to increase rapidly up to $\lambda = 2$ after which point only incremental increases were obtained by increasing λ . This result suggests the possibility of using a two stage reactor system which also has been suggested by others[11]. One scheme could be operating with a λ of ~ 2 in the first stage and using a higher λ in the second stage to get almost complete conversion of the CO.

Since the maximum selectivity occurs for $\lambda = 1$, which is the stoichiometric amount to oxidize CO to CO₂, and diminishes from thereon, while simultaneously increasing conversion suggests the rate limiting step is the oxidation of CO. Since the conversion only incrementally increases after $\lambda = 2$ while selectivity decreases more dramatically at that point, increasing O₂ does not efficiently oxidize the CO after stoichiometric amounts have been introduced. Therefore, variables other than stoichiometry, such as reactor design or catalyst formulation must be investigated.

The heat of adsorption of CO on supported platinum is known to be a strong function of platinum particle size with higher strength of adsorption on smaller particles [24]. Therefore, a preliminary study was made on the effect of platinum loading on catalyst activity and selectivity. The results are shown in Figure 9. It was observed that the operating temperatures for maximum catalyst activity and selectivity were a function of the catalyst loading, with the maximum in activity and selectivity shifted to higher operating temperatures with lower loading as would be expected with a particle size effect. This preliminary study demonstrates the concept of using platinum loading to vary the optimum operating temperature along the length of the reactor. Modifying the catalyst activity by the use of promoters, alloying with other PGM, etc. may also be used to achieve a similar result.

A. Reactor Design Implications of Microlith

The discrete nature of the SCL-HCD catalyst substrate allows the staging of catalyst formulations (using different catalyst formulations on the individual SCL-HCD elements along the length of the bed) to optimize catalyst selectivity with the temperature rise of the exothermic reaction. This could potentially enable complete conversion in a single PROX reactor with high selectivity for CO oxidation. In order to achieve this, kinetics will have to be determined over a range of temperatures, space velocities and reactant and product compositions. This could enable targeted catalyst formulations to be used throughout the reactor to achieve certain reactions.

Reactor operating parameters (e.g. reactor volume and pressure) were examined for an understanding of their contribution to the performance of the reaction. Microlith reactors have the equivalent pressure drop per unit conversion when compared to performance on standard monoliths at about 1/10th the volume. Hence high conversions can be achieved without a pressure drop penalty. The operating window for the reactor must also meet the requirement of near instantaneous startup times and load following capability. The reactor must therefore be responsive to changes in conditions within a time frame where those parameter changes are observed. For example, if flow rate changes on the order of seconds, the reactor must respond on the order of seconds to avoid over temperatures or excessive reactant breakthrough during those changes. All of these attributes can be categorized as transient response capability. Figure 10 shows the response of a sub-scale reactor using the supported Pt catalyst studied. A preliminary study of the transient response characteristics of the Microlith catalyst substrate was performed using approximately a 0.1" bed depth. The CO conversion across the bed was stabilized at ~ 80% at a total flowrate of 6 SLPM to yield a space velocity of 440,000 hr⁻¹. The flow was then instantly switched to 3 SLPM keeping the gas composition the same (response time of the mass flow controller is ~ 3 sec to 95% of new setpoint) and the CO conversion was monitored. After stabilizing at this condition for about 20 minutes the flow was switched back to 6 SLPM and allowed to stabilize at this condition. The change from 6 to 3 SLPM would be a simulated load change from 100% to 50% at $\lambda = 2.0$. While reaching the steady state condition required as much as 10 minutes, this was primarily due to the inability of the test rig to reach a steady feed gas temperature. Despite the limitations of the test rig, the tests indicated that (a) the bed temperature tracked the inlet or control temperature very closely (less than 1 second) and (b) variation in CO conversion was limited to $\pm 5\%$ (primarily due to lack of appropriate inlet temperature control). The preliminary data therefore suggests that a Microlith reactor sized for the maximum load conditions may be able to adequately handle transient loads with rapid response times.

The two most important aspects of the test are (a) the ability for the reactor to follow the changes in inlet temperature and (b) the ability for the reactor to maintain a high CO conversion during those transients and during the subsequent dampening period for the inlet temperature to reach stable conditions. Additionally the diffusion characteristics of the Microlith reactor along with very low thermal mass and high transport properties, especially for heat transport, enables this type of quick response without hot spots or reactant breakthrough to occur. Notice during the first change, near 21 minutes, the conversion and surface temperatures respond immediately and track exactly to the changes in inlet temperature while approaching steady state. The oscillations in the inlet temperature are an artifact of the way the experiment was done. The inlet setpoint was not adjusted during the flow change, which caused the initial drop then overshoot of temperature.

The various space velocities as a function of inlet temperature within the operating window were mapped out for the subscale reactor. Figure 11 shows the results of the tests in terms of CO conversion versus inlet gas temperature for a range of space velocities. As expected, the lightoff temperature increases and maximum conversion decreases with increasing space velocity. After maximum conversion has reached a peak, there is a gradual falloff in conversion, which is on the right side of the curves. This falloff could be due to a gradual shift in O₂ conversion with H₂ instead of only CO, which would cause a higher local temperature at the surface that would start reverse water gas shift reactions occurring. This type of performance begins to carve out an operating window for the PROX reactor in terms of inlet temperatures needed for various space velocities and the levels of conversion that can be obtained.

It can be seen that the inlet temperature needs to decrease as the space velocity decreases over a 2.5:1 turndown ratio. This type of operating scheme will need to be engineered properly in the sense that some systems may have a constant inlet temperature for a range of loads. A temperature drop would be possible by keeping the flow of coolant through a heat exchanger constant while the system turns down, where the design point for the flow will be to achieve the desired inlet temperature at 100% power. Therefore, when the fuel processor system is turned down, the amount of cooling the exchanger can do is

more per unit of process flow. This may lead to a simpler design in that heat exchanger flows do not need to be adjusted, which is one less parameter that needs feedback control.

When all the parameters going into making up the PROX reactor have been worked through once, such as selection of catalyst formulation, space velocity, operating window and pressure drop, a second iteration can begin. This iteration would be the first in a series of attempts to optimize the performance of the reactor either for a specific application or to enable the reactor to accommodate a few different applications. Improvements in catalyst formulation are usually considered the place where the largest impact could be obtained in that no rigorous algorithm exists to determine how various changes in catalyst formulation will impact performance. While it is known that higher ASI gives lower lightoff temperatures, there is little information about how various promoters or PGM alloys could effect lightoff, turndown and overall performance, including durability. These unknowns contrast the reactor design variables, which are generally known and understood. For example, the transport phenomena for the reactor is known, there are good correlations for packed beds (25,26) and monoliths (27) and PCI has developed a very accurate model for Microlith(15,16) reactors. This leads to a rigorous analysis of mass and heat transfer throughout the reactor and how changes in inlet and bed temperature and space velocity will effect heat exchanger duties and pressure drop. Because of these issues, iterations on catalyst formulation were first investigated to help widen the operation envelope of the reactor. Figure 12 shows the result of a second-generation catalyst formulation, which was developed from optimization of desired attributes from the above formulations. The results show the ability for the reactor to lightoff nearly 60°C lower in temperature and has a broader operating window than the first-generation formulation as evidenced by the flatter conversion peak. In addition, this new formulation did not significantly impact the maximum conversion or selectivity. The maximum conversion here is 90% versus 93% and selectivity is 38% versus 42% when comparing the second-generation to the first-generation catalyst.

4. CONCLUSION

A study was done to determine the effect of a short contact time, non-equilibrium reactor, termed Microlith, on preferential CO oxidation reactions. An understanding of the competing reactions present is critical to successful reactor design. An operating window was defined for the reactor in terms of space velocity, inlet temperature, CO conversion and selectivity and O₂ stoichiometry, λ . In addition, a series of PGM catalysts were examined, resulting in a supported Pt catalyst being chosen for the reactor design studies. A reactor was demonstrated, with an operating window encompassing space velocity = 440,000 hr⁻¹, inlet temperature of 160°C and $\lambda = 2.4$, which can be used in fuel cell automotive applications and meet the PNGV targets.

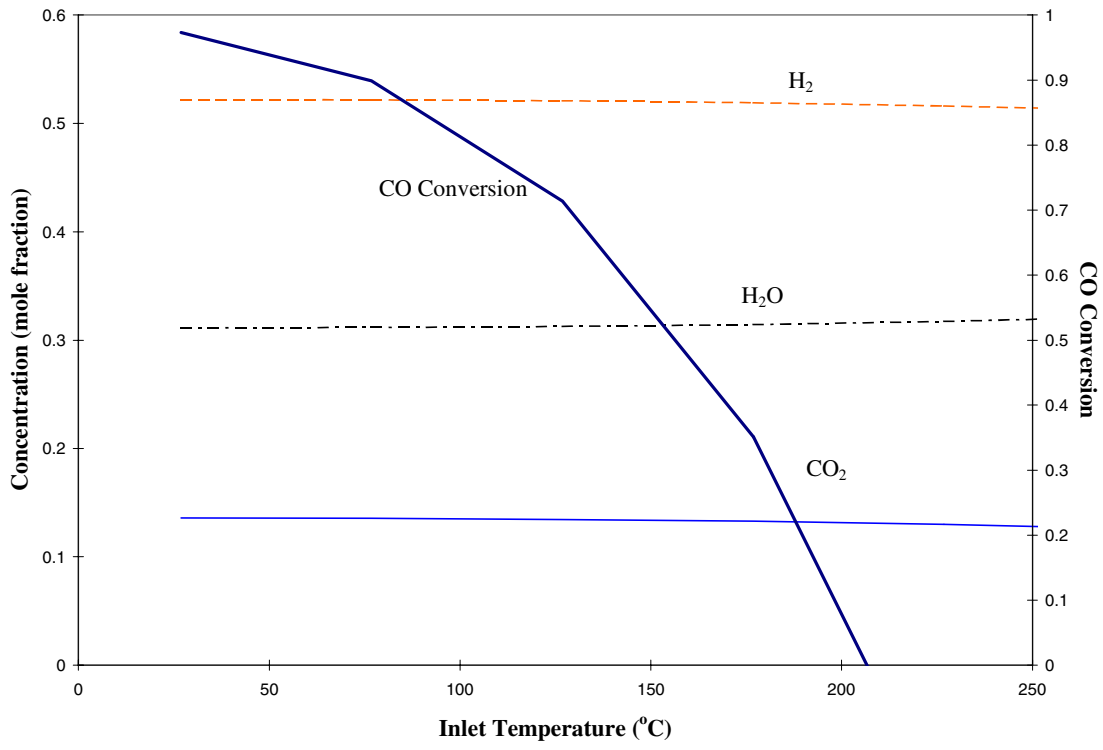


Figure 1: Equilibrium Calculations for shifted reformat.

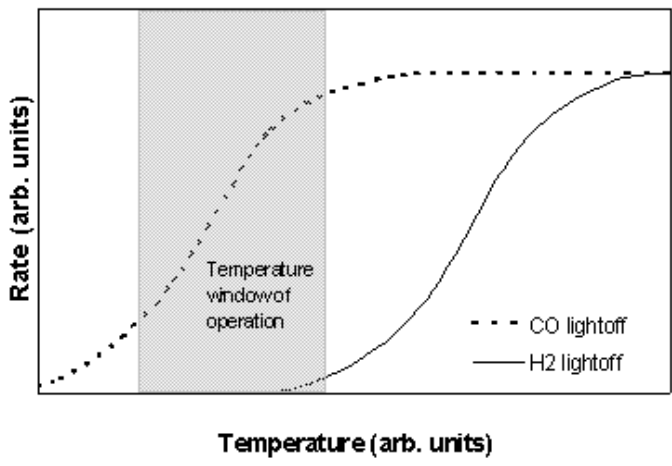


Figure 2: Schematic illustration of CO and H₂ lightoff on PROX catalyst.

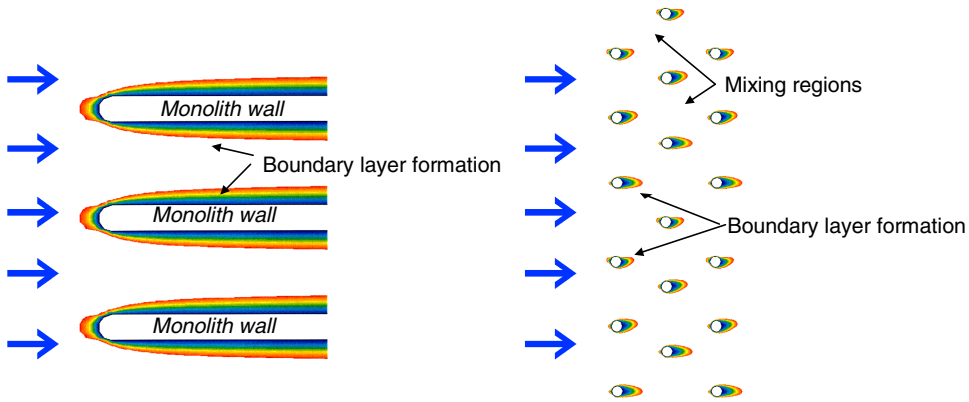


Figure 3. Results of CFD calculation of the boundary layer formed around a conventional monolith and Microlith metal monoliths in series (6.1 m/s air flow at 450 °C). Note: the different colors show the velocity profile along across the boundary layer (increasing from blue to red). The uncolored region represents essentially bulk flow conditions.

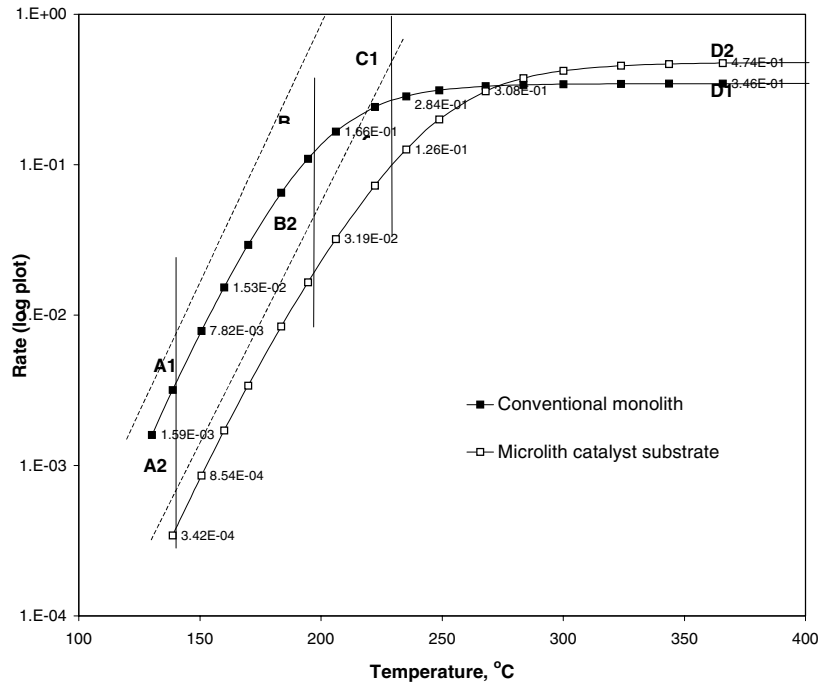


Figure 4. CO Conversion on supported Pt catalyst modeled using parameters from ref. [28]. This analysis compares a conventional 400 cpsi monolith with a Microlith reactor less than 1/10th the size.

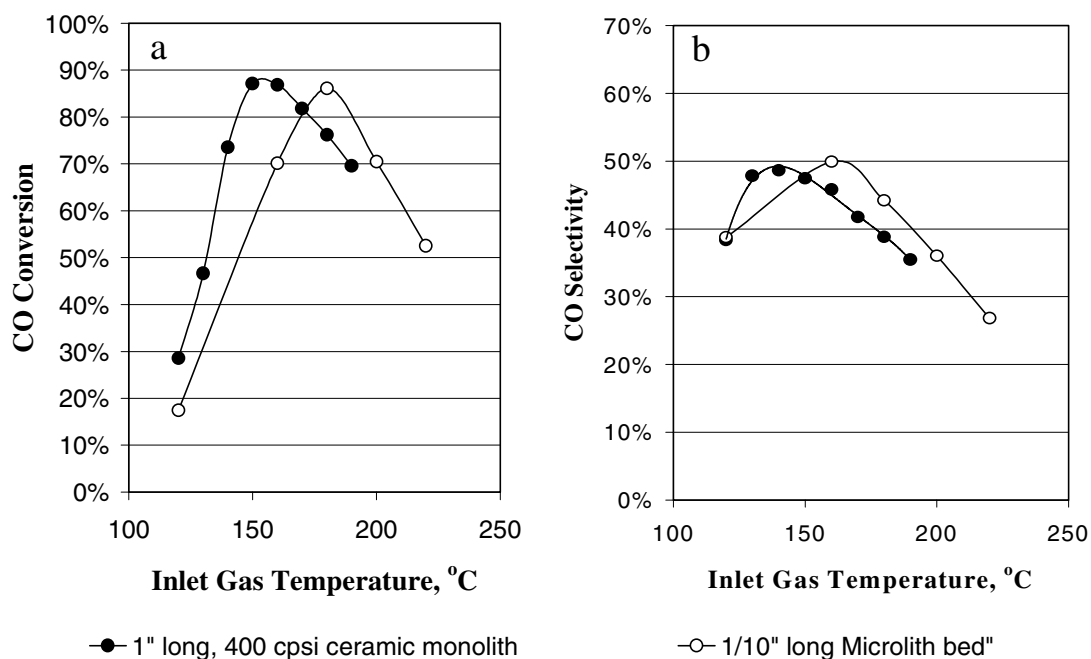


Figure 5. CO conversion and selectivity for a 0.1 in. deep Microlith reactor and a 1 in. deep, 400 cpsi ceramic monolith sample incorporating the same catalyst and washcoat with space velocities of 440,000 hr⁻¹ and 44,000 hr⁻¹ respectively.

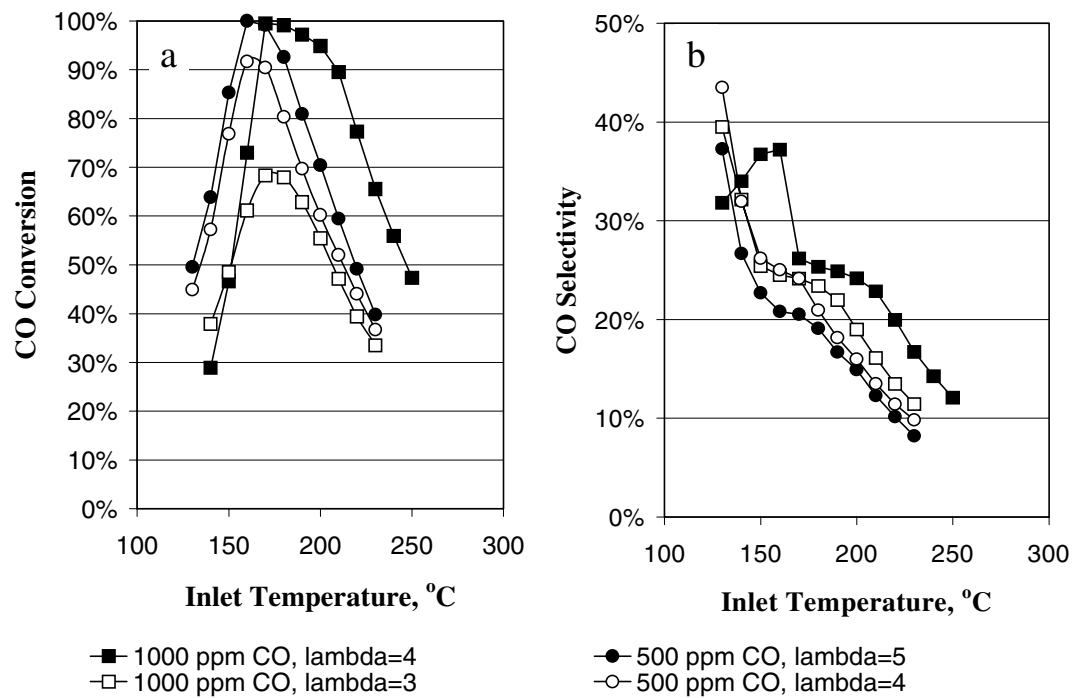


Figure 6: Comparison between conversion (a) and selectivity (b) for different CO inlet concentrations and λ using a supported Pt catalyst with ASI = 17.

Table 1:

Parameter	Microlith catalyst substrate	400cpsi Monolith
k_c , m/sec ^[28, 29]	1.30	0.10
A, m ²	0.37	3.46

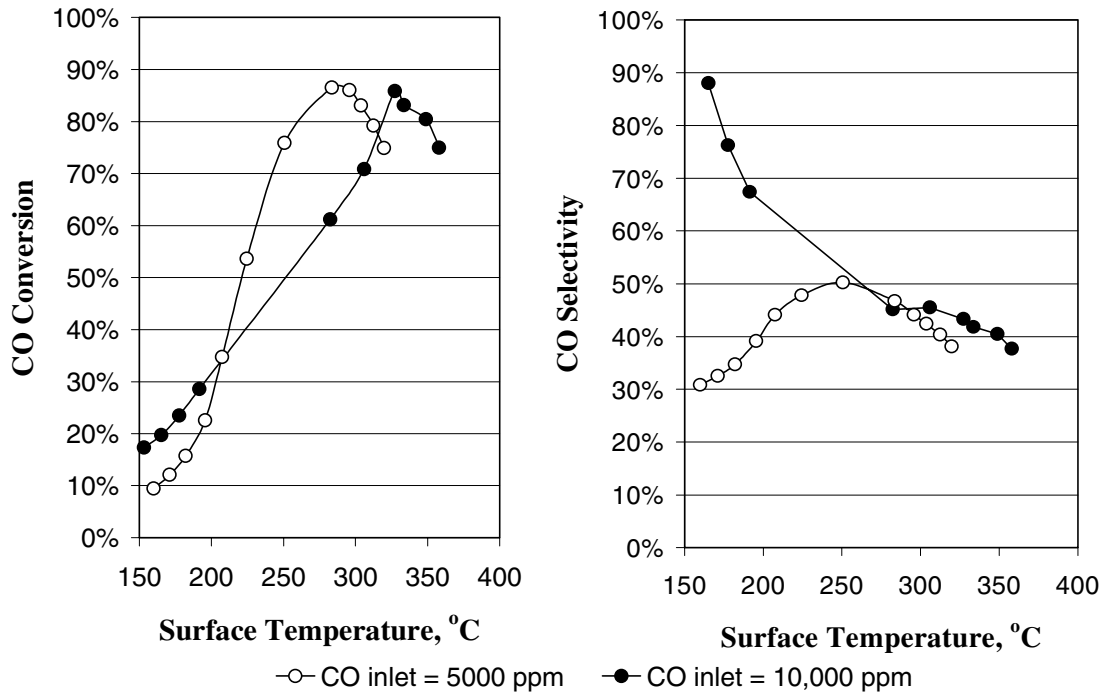


Figure 7. A Comparison of lightoff and maximum conversion versus temperature for high inlet CO concentrations. Study done using $\lambda=2$ for the same supported Pt catalyst as in Figure 6.

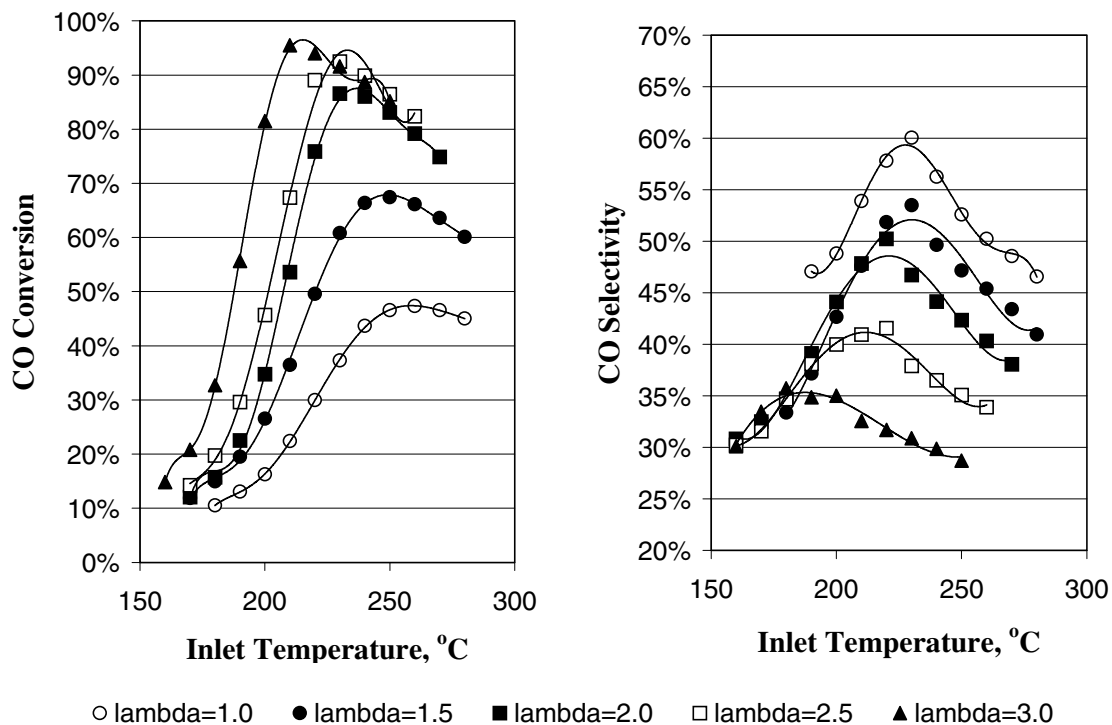


Figure 8. Comparison of oxygen concentration from stoichiometric amounts ($\lambda=1$) to 3 times in excess to begin to elucidate the mechanism of CO oxidation.

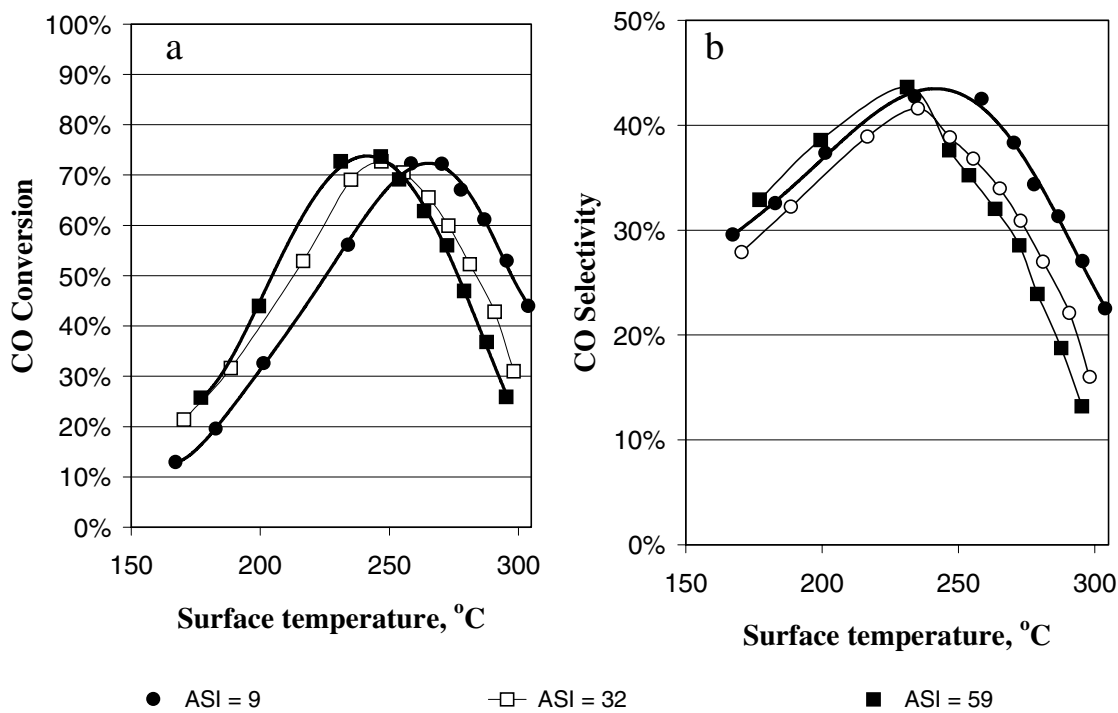


Figure 9. Loading study to begin to determine the effect ASI has on catalyst performance in terms of conversion (a) and selectivity (b) and its implications on reactor design.

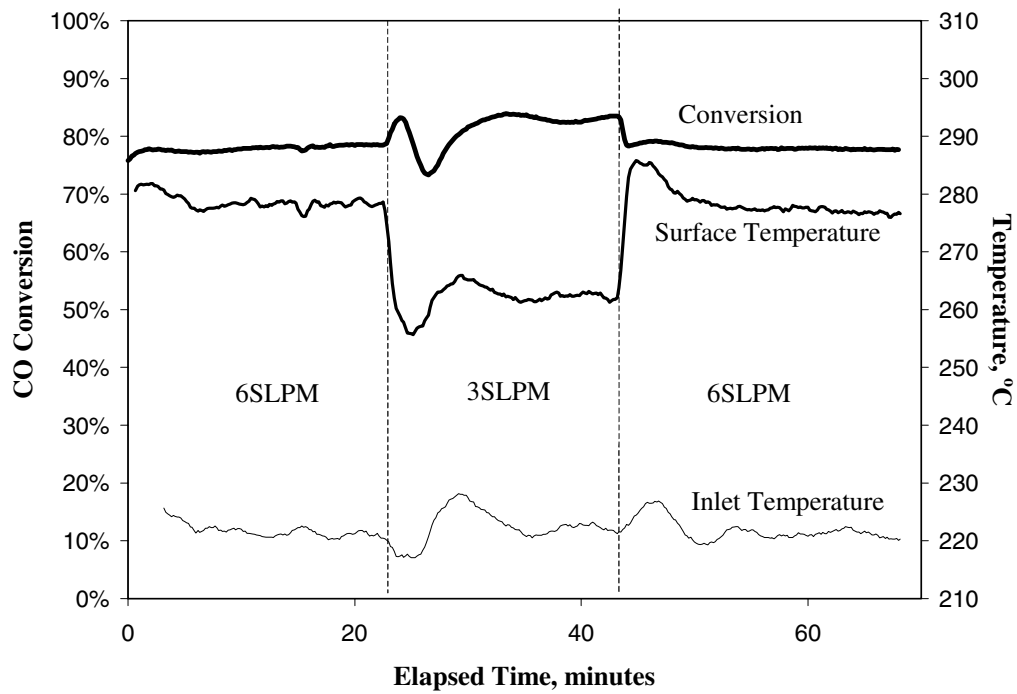


Figure 10. Transient or load following capability of the Microlith PROX reactor. Changes from 6 to 3 SLPM simulate load changes from 100% to 50%.

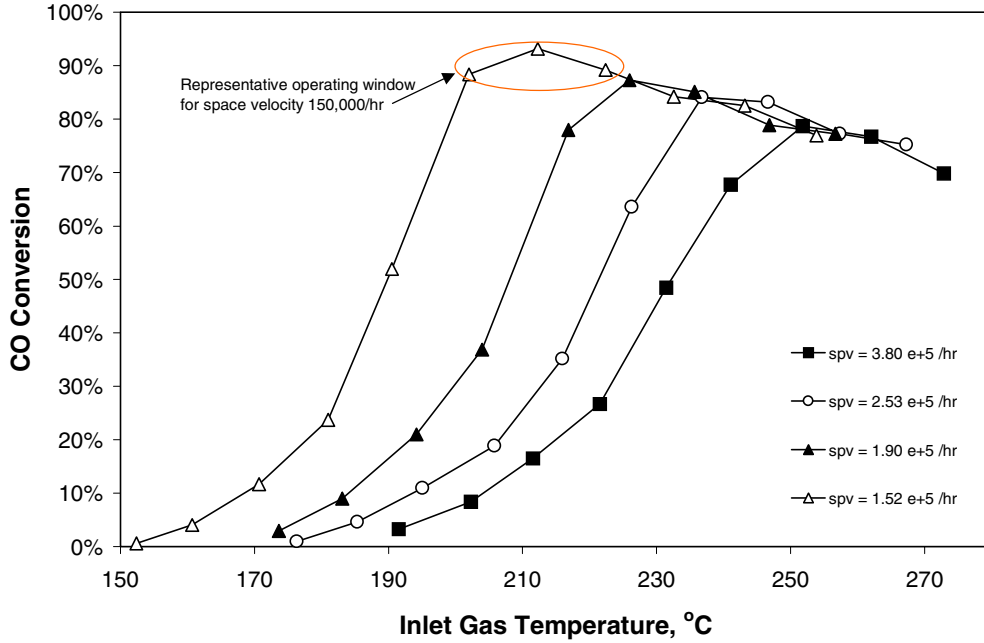


Figure 11. Results of conversion versus inlet temperature for various space velocities. Shows the range of inlet temperature operation for high CO conversion and the temperature of maximum conversion.

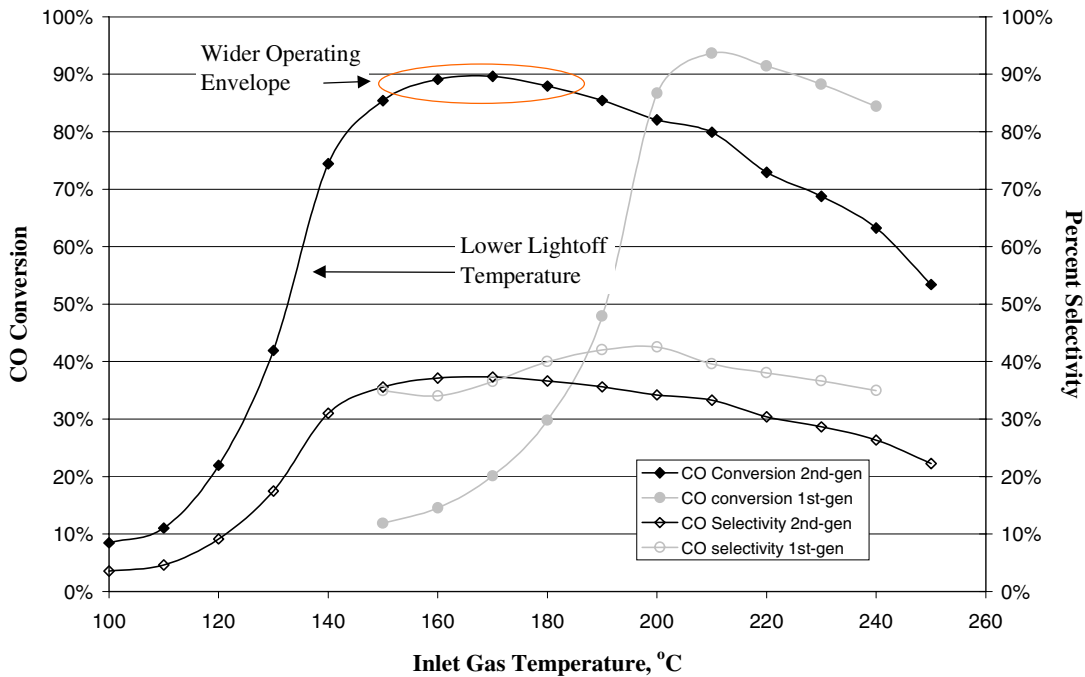


Figure 12. Comparison of first and second-generation catalysts for conversion and selectivity. The second-generation catalyst shows a marked improvement in terms of activity or lightoff and a wider temperature region for high CO conversion for various space velocities.

REFERENCES

1. L.D. Schmidt, *Stud. Surf. Sci. Catal.*, vol. 136, pp. 1-12, 2001.
2. Korotkikh, O., Farrauto, R., *Catal. Today* vol. 62. Pp. 249-254, 2000
3. Oh, S. H., Sinkevitch, R. M., *J. Catal.*, Vol. 142, pp. 254-262, 1993.
4. R. A. Lemmons, *J. Power Sources*, Vol. 29, p. 251, 1990.
5. Watanabe M., Uchida, H., Igarashi, H., and Suzuki, M., *Chem. Lett.*, Vol. 21, 1995.
6. Torres Sanchez, R. M., Ueda, A., Tanaka, K., *J. Catal.* Vol. 168, pp. 125-127, 1997.
7. Schubert, M., M., Gasteiger, H., A., and Behm, R., J., *J. Catal.* Vol. 172, p. 256, 1997.
8. Avgouropoulos, G., Ioannides, T., Matralis, H. K., Batista, J., Hocevar, S., *Catal. Lett.* VOL. 73 PP. 33-40, 2001.
9. Schubert, M. M., Kahlich, M. J., Feldmeyer, G., Huttner, M., Hackenberg, S., Gasteiger, H. A., Behm, R. J., *Phys. Chem. Chem. Phys.* Vol. 3 pp. 1123-1131, 2001.
10. Igarashi, H., Uchida, H., Watanabe, M., *Chem. Lett.*, No. 11, pp. 1262-1263, 2000.
11. Kahlich, M.J., H.A. Gasteiger, and R. J. Behm, *J. New Mat. Electrochem. Systems*, vol. 1 pp 36-46, 1998.
12. Igarashi, H., Uchida, H., Suzuki, M., Sasaki, Y., Watanabe, M., *Applied Catal. A, General*, Vol. 159, pp. 159-169, 1997.
13. Schubert, M.M., Kahlich, M.J., Gasteiger, H.A., Behm, R.J. *J. of Power Sources*, Vol. 84, pp. 175-182, 1999.
14. U.S. Patent 5,051,241 – William C. Pfefferle.
15. Roychoudhury, S., Muench, G., Bianchi, J.F., Pfefferle, W. C. and Gonzales, F., SAE Paper 971023, SAE International, Warrendale, PA, 1997.
16. Carter, R. N., Menacherry, P.V., Pfefferle, W. C., Muench, G. and Roychoudhury, S., SAE Paper 980672, SAE International, Warrendale, PA, 1998.
17. Gates B. C., "Catalytic Chemistry", pp. 224, John Wiley and Sons, New York, 1992.
18. Brown, L.,F., Los Alamos National Laboratory Report # LA-UR-01-1005
19. NIBBILKE REF
20. M.L. Brown, A.W. Green, G. Cohn and H.C. Anderson, *Ind. Eng. Chem*, vol 52, p 841, 1960.
21. R.M. Torres Sanchez, A Ueda, K. Tnaka and Haruta, *J. Catal.*, vol 168, p 125, 1997.
22. M.J. Kahlich, H.A. Gasteiger, and R. J. Behm, *J. Catal.*, vol. 182, p. 430, 1999.
23. G. B. Hoflund, S.D. Gardner, D.R. Schryer, B.T. Upchurch and E.J. Kielin, *React. Kinet. Catal. Lett.*, vol 58, pp.19-26, 1996.
24. Altamn, E.I. and Gorte, R.J., *J. Catal.*, vol. 110, p. 191, 1988.
25. McCabe, M.L., Smith, J.C., and Harriet, P., *Unit Operations of Chemical Engineering*, 4th Edition, McGraw-Hill, New York 1985.
26. Fogler, H.S., *Elements of Chemical Reaction Engineering*, 2nd Edition, Prentice Hall, Englewood Cliffs, NJ.
27. Cybulshi, A., and Mouliign, J.A., *Catal. Rev.-Eng.Sci*, Vol. 36, pp. 179-270, 1994.
28. Ullah, U., Waldram, S.P., Bennet, C. J.and Truex, T., *Chem. Eng. Science* Vol. 47, p. 2413, 1992.
29. Satterfield, C. N. and Cortez, D. H., *Ind. Chem. Fundam.*, Vol. 9, p.613, 1970.